

This Provisional PDF corresponds to the article as it appeared upon acceptance. Copyedited and fully formatted PDF and full text (HTML) versions will be made available soon.

BreakTrans: uncovering the genomic architecture of gene fusions

Genome Biology 2013, **14**:R87 doi:10.1186/gb-2013-14-8-r87

Ken Chen (kchen3@mdanderson.org)
Nicholas E Navin (nnavin@mdanderson.org)
Yong Wang (YWang33@mdanderson.org)
Heather K Schmidt (hschmidt@genome.wustl.edu)
John W Wallis (jwallis@genome.wustl.edu)
Beifang Niu (bniu@genome.wustl.edu)
Xian Fan (xfan3@mdanderson.org)
Hao Zhao (HZhao1@mdanderson.org)
Michael D Mclellan (mmclella@genome.wustl.edu)
Katherine A Hoadley (hoadley@med.unc.edu)
Elaine R Mardis (emardis@wustl.edu)
Timothy J Ley (tley@DOM.wustl.edu)
Charles M Perou (cperou@med.unc.edu)
Richard K Wilson (rwilson@genome.wustl.edu)
Li Ding (lding@genome.wustl.edu)

ISSN 1465-6906

Article type Software

Submission date 12 March 2013

Acceptance date 19 August 2013

Publication date 23 August 2013

Article URL <http://genomebiology.com/2013/14/8/R87>

This peer-reviewed article can be downloaded, printed and distributed freely for any purposes (see copyright notice below).

Articles in *Genome Biology* are listed in PubMed and archived at PubMed Central.

For information about publishing your research in *Genome Biology* go to

<http://genomebiology.com/authors/instructions/>

© 2013 Chen *et al.*

This is an open access article distributed under the terms of the Creative Commons Attribution License (<http://creativecommons.org/licenses/by/2.0>), which permits unrestricted use, distribution, and reproduction in any medium, provided the original work is properly cited.

BreakTrans: uncovering the genomic architecture of gene fusions

Ken Chen^{1,2*}, Nicholas E Navin^{1,4}, Yong Wang⁴, Heather K Schmidt³, John W Wallis³, Beifang Niu³, Xian Fan^{1,2}, Hao Zhao¹, Michael D McLellan³, Katherine A Hoadley⁵, Elaine R Mardis³, Timothy J Ley^{3,6}, Charles M Perou⁵, Richard K Wilson³ and Li Ding^{3,6*}

¹Department of Bioinformatics and Computational Biology, The University of Texas M.D. Anderson Cancer Center, 1515 Holcombe Blvd, Houston, Texas 77030 (USA)

²Department of Computer Science, Rice University, 6100 Main St, Houston, Texas 77251 (USA)

³The Genome Institute, Washington University School of Medicine, 4444 Forest Park Ave, St. Louis, MO 63108 (USA)

⁴Department of Genetics, The University of Texas M.D. Anderson Cancer Center, 1515 Holcombe Blvd, Houston, Texas 77030 (USA)

⁵Department of Genetics, University of North Carolina School of Medicine, 120 Mason Farm Road, Chapel Hill, NC 27599 (USA)

⁶Department of Medicine, Washington University School of Medicine, 660 S. Euclid Ave, St. Louis, MO 63110 (USA)

*To whom correspondence should be addressed. Email: kchen3@mdanderson.org and ld Ding@genome.wustl.edu

Abstract

Producing gene fusions through genomic structural rearrangements is a major mechanism for tumor evolution. Therefore, accurately detecting gene fusions and the originating rearrangements is of great importance for personalized cancer diagnosis and targeted therapy. We present a tool, BreakTrans, that systematically maps predicted gene fusions to structural rearrangements. Thus, BreakTrans not only validates both types of predictions, but also provides mechanistic interpretations. BreakTrans effectively validates known fusions and discovers novel events in a breast cancer cell line. Applying BreakTrans to 43 breast cancer samples in The Cancer Genome Atlas identifies 90 genomically validated gene fusions. BreakTrans is available at <http://bioinformatics.mdanderson.org/main/BreakTrans>

Keywords

Gene fusion, genomic structural rearrangement, breakpoint graph, genome architecture, whole genome sequencing, whole transcriptome sequencing

Rationale

Many cancers are driven by pathogenic expression of mRNA fusion transcripts produced by genomic structural rearrangements (GSR) in tumor cells. Classic examples include *BCR-ABL1* in CML [1], *PML-RAR α* in APL [2], and *TMPRSS2-ERG* in prostate cancer [3]. These fusions can arise from not only simple translocations of two distal genomic loci [4] but also complex GSRs that involve multiple distal loci [5-8]. Accurately identifying these pathogenic transcripts and the originating GSRs will have a major impact in personalized cancer diagnosis and targeted therapy [4, 9].

Since 2008, next generation sequencing (NGS) technologies have been applied to identify GSR breakpoints and gene fusions. Many bioinformatics tools such as BreakDancer [10], VariationHunter [11], and CREST [12] have been developed to detect GSRs from whole genome sequencing (WGS) data. These tools predict individual genomic breakpoints by searching for clusters of abnormally mapped reads. Although generally useful, they often produce an appreciable number of false positives and false negatives introduced by insufficient coverage, short insert size, misaligned reads, GC content bias, base calling errors, and repeats [13]. Limitation in data quality and the complexity of rearrangements make it a challenging task to infer the structure of complex GSRs (or so-called genome architecture) from predicted individual breakpoints [14, 15]. Meanwhile, many tools such as Tophat-fusion [16], deFuse [17], MapSplice [18], and BreakFusion [19] have been developed to detect gene fusions from whole transcriptome sequencing (WTS) data. These tools are algorithmically similar to their genomic counterparts although they have more emphasis on mapping and ascertaining novel sequence junctions produced by mRNA-splicing and are more robust in modeling the coverage (expression). Again, these tools are associated with various types of false positives and false negatives [20] and often do not have good concordance.

When both WGS and WTS data are available, we can compare them to identify GSRs that lead to gene fusions. Because of the technical independency of these two data sources, their comparison can serve as a form of validation. In addition to improving results, mapping fusions to GSRs also elucidates the mechanistic origins of these fusions and their potential clinical values. However, such analysis is complicated by several factors. First, because of mRNA splicing, the genomic breakpoints responsible for a fusion may not be located near the fusion boundaries. Second, a fusion may be produced via multiple genomic breakpoints that join segments from distal regions of the genome. Several types of such complex GSRs have been recently revealed by WGS in various cancer types [5-7, 21, 22]. Third, not all GSRs produce new genes that can be transcribed. The properties (e.g., location, type, and strand) of individual GSR breakpoints and the potential of producing valid open reading frames from existing genes need to be accounted for so as to produce biologically meaningful results. Fourth, current NGS data have limited power to accurately determine the genomic architectures of underlying alleles [23]. The technological limitations in resolving repeats and phase and the lack of physical coverage make it difficult to derive correct results.

To sufficiently address these challenges, systematic approaches are in demand. Recently, two bioinformatics tools, Comrad [24] and nFuse [25] were developed to address this challenge. Both tools align raw WGS and WTS reads while simultaneously corroborating fusions and GSRs. As an early effort, Comrad only maps a single fusion breakpoint to a single genomic breakpoint through the application of a set of *ad hoc* rules. As an update, nFuse maps fusion breakpoints to complex GSRs using a graph-theoretic approach. A design advantage of these tools is that they can account for ambiguous read alignment and therefore potentially minimize errors caused by misalignments. However, Comrad was only able to analyze low-path WGS data that have limited power in discovering GSR. Moreover, the self-contained design restricts them from examining hypotheses produced by other well-attested algorithms such as Tophat-fusion, MapSplice, BreakDancer and CREST.

To overcome these limitations, a modularly designed tool that focuses on mapping fusions to GSRs without re-performing breakpoint discovery may better serve the analytical demand and utilize existing resources. In this paper, we present such a bioinformatics tool BreakTrans that integrates the results of various fusion and GSR prediction algorithms and returns a set of genomically-validated fusions with their originating alleles.

Results

Overview of BreakTrans

BreakTrans is designed to map gene fusions predicted by a set of fusion prediction programs, such as deFuse, MapSplice, Tophat-fusion and BreakFusion, to GSR breakpoints predicted by a set of GSR prediction algorithms, such as BreakDancer, CREST, and VariationHunter (Figure 1 and **Methods**). BreakTrans includes 4 major steps: 1) parse and read in GSR and fusion breakpoints produced by front-end tools, 2) construct a genomic breakpoint graph from GSR breakpoints, 3) search for genomic alleles (paths in the breakpoint graph) that support fusion hypotheses, and 4) output validated fusions and associated genomic alleles.

Cell-line SK-BR-3

We applied BreakTrans to study the genome and transcriptome of SK-BR-3, a breast cancer cell-line. We downloaded WTS data from the NCBI Sequence Read Archive [SRA:SRP003186]. We collected fusion breakpoints from 3 different sources. First, we analyzed the WTS data using Tophat-fusion-0.1.0 (Beta) and obtained 27 fusion breakpoints. Second, we analyzed the data using BWA [26] and BreakDancer [10] with NCBI human assembly build36 as the reference. From this analysis, we obtained 2,065 putative fusion breakpoints that contained 6 of the 10 known fusion genes in SK-BR-3 (Table 1) [27]. To further increase sensitivity, we included 28 Tophat-fusion breakpoints and 1,395 deFuse breakpoints that were previously published using the same set of WTS data [28]. This set included 7 known fusion genes. Altogether, 3,498 unique fusion breakpoints were obtained (Additional File 1), that included 7 of 10 known fusion genes. To obtain a set of genomic breakpoints, we generated 80 fold 100 bp paired end WGS reads (Illumina) from genomic DNA [SRA:SRP028176]. We mapped the WGS reads against build36 reference using BWA and performed BreakDancer and CREST [29] analysis. BreakDancer and CREST predicted 23,567 (>1,000 bp) and 18,048 genomic breakpoints, respectively. Altogether, 41,615 unique genomic breakpoints were obtained (Additional File 2).

We ran BreakTrans-0.0.6 on these two sets of fusion and genomic breakpoints and obtained a set of 40 redundant fusion breakpoints that are supported by genomic alleles (Additional File 3). These fusion breakpoints are redundant (in location) due to our inclusion of multiple sources at variable nucleotide resolutions. Altogether, these 40 breakpoints nominated 8 unique fusion genes (Table 1), including 6 of the 10 known fusion genes and 2 novel ones.

Of the 4 known fusion genes that we missed, *DHX35-ITCH* and *NFS1-PREX1* were likely due to insufficient coverage of the transcriptome, as indicated by a previous study [28]. *CYTH1-EIF3H* was due to insufficient coverage of the genome: neither BreakDancer nor CREST detected any genomic rearrangements that can be associated with this fusion. Although the WGS data we used have great sequence coverage (80 fold), its physical coverage is quite limited: the average insert size is only 211 bp with a read length of 100bp. *CSEIL-ENSG00000236127* has become obsolete because of the exclusion of *ENSG00000236127* from the Ensembl database, as previously explained [28]. BreakTrans was able to validate all known fusions with sufficient coverage from this dataset, indicating its high sensitivity.

For comparison purpose, we ran nFuse-0.1.4 on the same WTS and WGS datasets using default parameters. Among the 1,994 predicted fusion breakpoints (Additional File 4), only 2 of the known fusion genes (*ANKHDI-PCDH1* and *SUMF1-LRRFIP2*) were identified.

The two novel fusion genes *PREX1-CPNE1* and *MTBP-SAMD12* detected by BreakTrans were both nominated by deFuse and are both likely to be valid. *PREX1*, *CPNE1*, and *SAMD12* have respectively fused with other genes in breast cancer cell-lines: *NFS1-PREX1* in SK-BR-3, *CPNE1-PI3* in BT-474 [27], and *PHF20L1-SAMD12* in HCC1954 [25, 30]. The *PREX1-CPNE1* fusion occurs precisely at the known exon boundaries (see Additional File 5, Figure S1).

Genomic regions containing these genes underwent substantial copy number alteration (CNA) (Figure 2), which have been shown to co-occur with gene fusions [27]. Furthermore, both *PREX1* and *MTBP* have been previously implicated in breast cancer progression [31-33].

These 8 fusion genes were supported by 9 unique alleles, as shown by the breakpoint paths in Table 1. Six of the 9 alleles contain one unique genomic breakpoint, representing the simplest way of generating fusion. The allele that encodes *PREX1-CPNE1* contains two breakpoints, which connect DNA segments from 3 different genes on chromosome 20. Included are the first 3 exons of *PREX1*, an intronic segment of *PHF20*, and the last 3 exons of *CPNE1* (Figure 3a). These breakpoints are highly supported by WGS data: 17 soft-clipped reads were found at the *PREX1-PHF20* breakpoint and 18 at the *PHF20-CPNE1* breakpoint (see Additional File 5, Figures S2-S5). They also overlap precisely with CNA boundaries (Figure 2a). The *MTBP-SAMD12* allele contains 5 unique breakpoints, all located in a single complex amplicon on chromosome 8. At least 3 breakpoints clearly coincide CNA boundaries (Figure 2b) with clusters of soft-clipped reads identified (see Additional File 5, Figures S6-S9). The breakpoint path indicates an inverted duplication, a type of genomic rearrangement that has been commonly observed in breast cancer cell-lines [21]. The *WDR67-ZNF704* fusion was supported by two different alleles, containing 3 breakpoints and 1 breakpoint, respectively. These breakpoints also coincide the boundaries of 2 distal amplicons on chromosome 8 (Figure 2c) with soft-clipped reads identified (see Additional File 5, Figures S10-S11).

To validate these novel fusion breakpoints, we generated two independent paired end RNA-seq datasets (SKBR3-1 and SKBR3-2) (76 bp read length) using the SK-BR-3 lines in our lab [SRA:SRP028176]. Both *PREX1-CPNE1* and *MTBP-SAMD12* were rediscovered at identical breakpoints using Tophat-fusion and BreakFusion, together with 9 of the previous known fusions (Additional Files 6 and 7). Note that both novel fusions were originally nominated using publically available RNA-seq data (50 bp read length) [SRA:SRP003186] by deFuse [28], which employs alignment and fusion-calling algorithms very different from either Tophat-fusion or BreakFusion. Such independence in the data and in the analytical approaches supported that both novel fusions predicted by BreakTrans are real biological events. Interestingly, we also re-

identified the genomic *PREX1-PHF20* breakpoint in one of the RNA-seq datasets (SKBR3-2) (Additional Files 7), which validated the existence of this breakpoint in the pre-mRNAs. We further validated a set of associated genomic breakpoints using polymerase chain reaction (PCR) (Additional File 8). If these genomic breakpoints were real, we should be able to observe PCR bands at expected DNA amplicon sizes. Out of the 6 breakpoints that we were able to design primers for, 4 amplicons had very clean bands (Figure 3b), which included both of the 2 breakpoints for *PREX1-CPNE1*, 1 for *MTBP-SAMD12* and 1 for *WDR67-ZNF704*. Interestingly, two different PCR bands were observed at one of the *WDR67-ZNF704* breakpoints (Figure 3b), consistent with our prediction that the *WDR67-ZNF704* fusion is associated with two different genomic alleles.

BreakTrans analysis of TCGA breast cancer WGS and WTS datasets

We applied BreakTrans to 43 breast cancer samples with both WTS and WGS data from the cancer genome atlas (TCGA, 12/30/2012)[34]. mRNA fusion breakpoints were nominated by BreakDancer by identifying clusters of read pairs that span different genes from the MapSplice [18] produced WTS BAM files. The genomic breakpoints were detected by two programs BreakDancer and SquareDancer (Chen et al., unpublished), which examine discordant read pairs and soft-clipped reads respectively. Together, we obtained a set of 156,955 redundant mRNA fusion breakpoints (an average of 3,650 per sample) and another set of 305,743 genomic breakpoints (an average of 6,794 per sample). We applied BreakTrans on these sets of breakpoints in conjunction with gene models specified in TCGA Genome Annotation Format (GAF) version 2.1, provided by the University of California Santa Cruz.

BreakTrans identified 177 redundant fusion breakpoints with convincing genomic evidence, which corresponded to 90 unique sample gene pairs (Additional File 9).

None of the fusions was found to be recurrent with identical gene pairs, suggesting a high level of heterogeneity in breast cancer as consistently demonstrated by previous studies [35]. However, we found a set of genes that recurrently partnered with others: *CBX3*, *C15orf57*, *BCAS3*, *RARA*,

USP15, PTPRN2, USP32, FBXL20, SNX27, WIPF2, NFI and *RAD51C*. Notably, the *USP* family members (*USP13, USP15, and USP32*) were frequently involved (in 5 fusions). Several fusions involved a kinase at the 3' end and are potentially viable therapeutic targets: *USP13-PIK3CA, GPR160-PRKCI, and FBXL20-TLK2*. Among the 43 samples, 33 were found to have more than 2 gene fusions with one (A09I) containing 10 fusion genes. This sample A09I also demonstrated extensive genomic instability with many copy number alterations, including focal amplification of over 60 folds (see Additional File 5, Figure S12).

Most of the 90 fusions (83.3%) involved one genomic breakpoint and 2 distal loci. The rest involved multiple genomic breakpoints. For example, the *NFI-NLE1* fusion in A09I involved 2 breakpoints and 3 genes: *NFI, CA0* and *NLE1* (see Additional File 5, Figures S13-S18), the *PPP1R1B-PIPOX* fusion in A0D1 involved 3 breakpoints and 3 genes: *PPP1R1B, NOS2* and *PIPOX* (see Additional File 5, Figures S19-S27), and the *PPP3R1-TTC27* fusion in A0YG involved 3 breakpoints and 4 genes: *PPP3R1, USP34, LTBP1* and *TTC27* (see Additional File 5, Figures S28-S37). Both *NFI-NLE1* and *PPP1R1B-PIPOX* occurred on the chr17q hotspot with GSR boundaries precisely overlapping CNA boundaries (see Additional File 5, Figures S12, S14, S20 and S21). *PPP3R1-TTC27* occurred on chr2 and was evidently associated with chromothripsis (see Additional File 5, Figures S29-S31) [6].

To prove the validity of BreakTrans predictions, we performed PCR validation on 20 genomic breakpoints (Additional File 10), including 9 that were associated with the above 3 multi-breakpoint fusions and 11 that we randomly selected from 9 samples. Out of these 20 breakpoints, 15 were validated as somatic, 1 as germline, and 4 as wild-type (see Additional File 11 and Additional File 5, Figures S38-S41). Further capillary sequencing of the PCR products confirmed the existence of one more breakpoint (see Additional File 5, Figure S42). Among the validated breakpoints were both of the 2 breakpoints underlying *NFI-NLE1*, all of the 3 breakpoints underlying *PPP3R1-TTC27*, and 2 of the 3 breakpoints underlying *PPP1R1B-PIPOX*.

Discussion

In this work, we presented a novel bioinformatics approach BreakTrans that systematically maps detected gene fusions to novel genomic alleles produced by GSRs, thereby validating both sets of hypotheses and providing mechanistic interpretation to validated fusions.

Our analysis and experimental validation indicated very high specificity of BreakTrans. The true specificity is likely higher than our estimation (60-80%), given the difficulties in performing PCR validation in repetitive regions.

Our results indicated that BreakTrans could achieve higher sensitivity through integration of multiple predictors without demonstrably increasing false positive rate. This is particularly important for current practice as individual predictors tend to be conservatively configured to achieve individually low false positive rates at the cost of increasing false negative rates. This phenomenon is particularly evident in our SK-BR-3 analysis, where we observed a large proportion of calls unique to a predictor. Conventional strategies that summarize results based on majority rules have been shown helpful in reducing false positives [36]. However, the further loss in sensitivity was usually not characterized. Applying BreakTrans to integrate multiple call sets is clearly a different and more effective strategy, as it integrates additional data. Indeed, the two novel fusions in the SK-BR-3 set were only nominated by deFuse and would have been eliminated if a simple consensus approach were taken. Our modular design allowed users to utilize their favorite predictors and include hypotheses from any source (e.g., literature). This feature relieves users from trying to determine the best predictors and post-processing strategies for their data, a non-trivial task.

Another contribution of our work is that we proposed a convention (breakpoint string) to represent individual breakpoint and breakpoint graph, as well as simple or complex alleles that encompass one or more breakpoints. This allows reporting and communicating large number of complex hypotheses in a concise and accurate way, an important requirement for large-scale

sequencing and clinical sequencing effort [37]. It also relieves researchers from manually piecing together alleles from individual breakpoints, a complex and error-prone task.

Our current version does not contain a scoring system to characterize the confidence of output fusions and alleles. This is mainly due to the complexity in integrating heterogeneous predictions from different sources, which are associated with heterogeneous scoring systems and precision.

With this version in place, we are actively working on approaches to rescore breakpoints and alleles using a genotype-likelihood framework [13, 36], which will be implemented into the future version of BreakTrans.

Although BreakTrans can effectively eliminate false breakpoints by leveraging the independence of WGS and WTS data and the existing knowledge of human transcriptome, the quality of the results is clearly dependent on the quality of the input. If a large number of false breakpoints were included and true breakpoints excluded, any approach will have difficulty deriving correct answers. Improving breakpoint accuracy itself is a non-trivial task given the complexity of the cancer genome and the limitation of NGS [13]. Therefore, it is important to apply modular design that allows problems and efforts to be distributed. BreakTrans makes it possible to separate the problem of breakpoint integration from that of breakpoint identification. Further improvement in either area will synergistically improve the final results.

Similar to other programs, BreakTrans requires sufficient coverage on both genomic and transcriptomic breakpoints to validate an event. Failure to validate an event does not necessarily negate its existence. This is a fundamental problem in analyzing heterogeneous tumor samples that often contain multiple clones of tumor cells [38], i.e., sub-clonal breakpoints may not receive sufficient coverage from standard bulk sample sequencing. However, as NGS continues evolving and its cost continues reducing, it becomes increasingly feasible to obtain deep coverage on both the genome and the transcriptome of sub-clonal cell populations [38] or even single cells [39].

Summary

We have developed a bioinformatics tool BreakTrans that systematically maps gene fusions to GSRs, an application that is important for molecular diagnosis and targeted therapy. Instead of re-performing breakpoint discovery, BreakTrans integrates breakpoint hypotheses from various sources using a novel breakpoint graphic approach. Our examination using the WGS and WTS data from a breast cancer cell-line SK-BR-3 indicates that BreakTrans has achieved higher sensitivity and specificity than existing approaches. Applying BreakTrans on the 43 breast cancer samples in TCGA, we have identified a set of “genomically validated” gene fusions that are promising for further functional study. As sequencing coverage continues to increase, we anticipate wide application of BreakTrans in both research and clinical settings.

Methods

Representing genomic breakpoints

Existing GSR detection programs such as BreakDancer and CREST predict individual breakpoints from clusters of abnormally aligned paired-end reads or soft-clipped reads. Each breakpoint represents a joining of two non-adjacent DNA segments (break-ends) that are adjacent in the reference genome. These breakpoints can be created by either simple genomic rearrangements such as deletion, insertion, and duplication, or complex genome rearrangements such as chromothripsis or close-chain translocation that creates multiple breakpoints [5-7, 25].

The resulting relationship between the two break-ends in the subject genome is called novel adjacency, as it does not exist in the reference genome. Such breakpoint can be represented using a graphic representation known as breakpoint graph [40]. Here, we define a breakpoint representation in the same vein but is more compact to use in our context. We define a “breakpoint string” to specify exactly how two DNA break-ends are joined together at the breakpoint (Figure 4). A breakpoint string consists of two break-ends: an in-end and an out-end. The in-end represents the end point of a DNA segment before entering the breakpoint. The out-end represents the start point of another DNA segment after exiting the breakpoint. The ends are directional (double stranded). We use “+” to represent positive strand and “-” to represent the negative strand. Each break-end is uniquely specified by a reference genomic coordinate x (consisting of a chromosome and a position) and a direction. We use a score f to quantify the confidence of the existence of the breakpoint. Popularly used scores include the number of reads or read pairs spanning the breakpoint or a genotype likelihood [41]. For notational convenience, we use a vertical bar ‘|’ to represent the connection between an in-end and an out-end.

The definitions above allow us to specify breakpoints produced by various types of genomic structural rearrangements in a consistent and concise format (e.g., $x+f/y+$). We further define four types of intra-chromosomal rearrangement breakpoints: “null”, “jump”, “inverse”, and “repeat”

(Figure 4a-d). A “null” breakpoint represents no breakpoint between x and y and the sequence between them are identical to the reference genome. We use a special score $f=0$ to denote such “null” breakpoint. A “jump” breakpoint joins together two non-adjacent segments on the same strand and skip the sequence between x and y . A breakpoint resulting from a deletion can be represented as a “jump”. An “inverse” breakpoint joins together two non-adjacent segments in opposite strand/orientation. It can represent breakpoints produced by inversions or inverted duplication. Finally, a “repeat” breakpoint connects x back to an upstream position y on the same strand. It can represent breakpoints produced by tandem duplication. Similarly, we can use breakpoint string to represent an inter-chromosome breakpoint, resulting from 4 different ways of joining the break-ends (Figure 4e-h). Taken together, breakpoint strings defined by our rules can encode most if not all rearrangement breakpoints. Similar to a DNA, a breakpoint string can be reverse-complemented by swapping the positions of x and y and flipping the orientations, i.e., $x+3|y+$ is identical to $y-3|x-$ albeit on the opposite strand. This feature allows us to encode breakpoints as undirected edges while enabling strand-aware search.

Constructing breakpoint graph

All of the existing NGS structural variant detection software output breakpoints individually, representing aberrant adjacencies in the subject genome. We can connect these breakpoints together to form a breakpoint graph, in which a node represents a genomic position that either terminates or leads a break-end, and an edge represents a breakpoint. The edges are undirected and are specific to various types of breakpoints, as specified by the breakpoint strings. In a polyploid genome, multiple alleles (chromosomes) are present. A node can thereby have multiple edges, each representing a different allele. Where no aberrancy detected, the subject genome is assumed to have the same allele as the reference genome. To represent a complete genomic architecture, edges with null breakpoints are added to represent the reference alleles that connect the breakpoints. Note that our representation is different from those used by nFuse, in which a node represents a break-end on a specified strand. In our case, a node only represents a position,

whether it leads or terminates a break-end on a specific strand depends on specifications on the connecting edges.

With a breakpoint graph being constructed, the task of decoding a chromosomal architecture is to identify paths that starts at the beginning and extends to the end of a chromosome. It is clearly a computationally challenging problem to identify correct paths in a graph that contain lots of nodes and edges.

Transcriptome guided search

To achieve accuracy and efficiency, it is desirable to simplify the graph. Rather than trying to decode the complete genome (global optimization), we can focus on expressed regions (local optimization). We ignore read-through events, which are out of our current scope, by disconnecting the reference allele (null edges) between the end nodes of neighboring genes. We can always restore these connections if read-through events become an interest.

Similar to a genomic breakpoint, a fusion (transcriptome) breakpoint predicted from mapping RNA-seq reads to the reference genome can be specified by two genomic positions x and y that locate in two different genes. To determine the underlying allele from which the fusion is transcribed, we first identify the nearest genomic breakpoints (x_0, y_0) downstream of x and y in the breakpoint graph. We then start at x_0 and perform recursive breadth-first search:

$p(x_0)=x_0+p(n(x_0))$, where the function $p(x)$ denotes the alleles starting at x , $n(x)$ denotes the set of nodes that connect to x and $+$ represents path extension. A path terminates if it hits either node y_0 or the end of a gene. This search algorithm returns all genomic alleles (or breakpoint paths) in the breakpoint graph that support a fusion hypothesis.

Data accessibility

BreakTrans code is available to download at

<http://bioinformatics.mdanderson.org/main/BreakTrans>.

The SK-BR-3 WGS and RNA-seq data are available at NCBI short reads archive [accession number SRP028176].

The TCGA breast cancer WGS and RNA-seq data can be obtained through dbGAP [accession number phs000178.v7.p6].

Abbreviations

GSR: genomic structural rearrangement; NGS: next generation sequencing; CNA: copy number alteration; bp: base pair; WGS: whole genome sequencing; WTS: whole transcriptome sequencing; TCGA: the cancer genome atlas;

Competing interests

The authors declare that they have no completing interests.

Authors' contributions

KC and LD conceived the study; KC designed and implemented the code; KC, JW, BN, MM, HZ and XF performed the analysis; NN provided SK-BR-3 WGS and RNA-seq data; YW and HS performed PCR validation, KC, NN and LD wrote the manuscript; LD, CP, KH, TL, RW and EM provided oversight and coordination of TCGA analysis. All authors read, revised and approved the final manuscript.

Acknowledgements

We thank Andrew Mcpherson for helping set up nFuse-0.1.4 and Tenghui Chen for assistance in fusion analysis. Nick Navin is a Nadia's Gift Foundation Damon Runyon-Rachleff Innovator (DRR-25-13). This work was supported in part by the National Cancer Institute (NCI) grant R01-CA172652-01 to K.C., R21CA174397-01 and R01CA169244-01 to N.N., National Human Genome Research Institute (NHGRI) grant U01-HG006517 and U54-HG003079, and the National Cancer Institute Cancer Center Support Grant P30-CA016672 and U24-CA143848. The results published here are in part based upon data generated by TCGA established by the NCI and NHGRI. Information about TCGA and the investigators and institutions who constitute the TCGA research network can be found at <http://cancergenome.nih.gov/>.

References

1. Rowley JD: **Letter: A new consistent chromosomal abnormality in chronic myelogenous leukaemia identified by quinacrine fluorescence and Giemsa staining.** *Nature* 1973, **243**:290-293.
2. Huang ME, Ye YC, Chen SR, Chai JR, Lu JX, Zhou L, Gu LJ, Wang ZY: **Use of All-Trans Retinoic Acid in the Treatment of Acute Promyelocytic Leukemia.** *Blood* 1988, **72**:567-572.
3. Tomlins S, Mehra R, Rhodes D, Cao X, Wang L, Dhanasekaran S, Kalyana-Sundaram S, Wei J, Rubin M, Pienta K, Shah R, Chinnaiyan A: **Integrative molecular concept modeling of prostate cancer progression.** *Nature Genetics* 2006, **39**:41-51.
4. Mitelman F, Johansson B, Mertens F: **The impact of translocations and gene fusions on cancer causation.** *Nature Reviews Cancer* 2007, **7**:233-245.
5. Berger MF, Lawrence MS, Demichelis F, Drier Y, Cibulskis K, Sivachenko AY, Sboner A, Esgueva R, Pflueger D, Sougnez C, Onofrio R, Carter SL, Park K, Habegger L, Ambrogio L, Fennell T, Parkin M, Saksena G, Voet D, Ramos AH, Pugh TJ, Wilkinson J, Fisher S, Winckler W, Mahan S, Ardlie K, Baldwin J, Simons JW, Kitabayashi N, MacDonald TY, et al: **The genomic complexity of primary human prostate cancer.** *Nature* 2011, **470**:214-220.
6. Stephens PJ, Greenman CD, Fu B, Yang F, Bignell GR, Mudie LJ, Pleasance ED, Lau KW, Beare D, Stebbings LA, McLaren S, Lin ML, McBride DJ, Varela I, Nik-Zainal S, Leroy C, Jia M, Menzies A, Butler AP, Teague JW, Quail MA, Burton J, Swerdlow H, Carter NP, Morsberger LA, Iacobuzio-Donahue C, Follows GA, Green AR, Flanagan AM, Stratton MR, et al: **Massive genomic rearrangement acquired in a single catastrophic event during cancer development.** *Cell* 2011, **144**:27-40.
7. Stephens PJ, McBride DJ, Lin ML, Varela I, Pleasance ED, Simpson JT, Stebbings LA, Leroy C, Edkins S, Mudie LJ, Greenman CD, Jia M, Latimer C, Teague JW, Lau KW, Burton J, Quail MA, Swerdlow H, Churcher C, Natrajan R, Sieuwerts AM, Martens JW, Silver DP, Langerod A, Russnes HE, Foekens JA, Reis-Filho JS, van 't Veer L, Richardson AL, Borresen-Dale AL, et al: **Complex landscapes of somatic rearrangement in human breast cancer genomes.** *Nature* 2009, **462**:1005-1010.
8. Rausch T, Jones DT, Zapatka M, Stutz AM, Zichner T, Weischenfeldt J, Jager N, Remke M, Shih D, Northcott PA, Pfaff E, Tica J, Wang Q, Massimi L, Witt H, Bender S, Pleier S, Cin H, Hawkins C, Beck C, von Deimling A, Hans V, Brors B, Eils R, Scheurlen W, Blake J, Benes V, Kulozik AE, Witt O, Martin D, et al: **Genome sequencing of pediatric medulloblastoma links catastrophic DNA rearrangements with TP53 mutations.** *Cell* 2012, **148**:59-71.
9. Welch JS, Ley TJ, Link DC, Miller CA, Larson DE, Koboldt DC, Wartman LD, Lamprecht TL, Liu F, Xia J, Kandoth C, Fulton RS, McLellan MD, Dooling DJ, Wallis JW, Chen K, Harris CC, Schmidt HK, Kalicki-Veizer JM, Lu C, Zhang Q, Lin L, O'Laughlin MD, McMichael JF, Delehaunty KD, Fulton LA, Magrini VJ, McGrath SD, Demeter RT, Vickery TL, et al: **The origin and evolution of mutations in acute myeloid leukemia.** *Cell* 2012, **150**:264-278.

10. Chen K, Wallis JW, McLellan MD, Larson DE, Kalicki JM, Pohl CS, McGrath SD, Wendl MC, Zhang QY, Locke DP, Shi XQ, Fulton RS, Ley TJ, Wilson RK, Ding L, Mardis ER: **BreakDancer: an algorithm for high-resolution mapping of genomic structural variation.** *Nature Methods* 2009, **6**:677-U676.
11. Hormozdiari F, Alkan C, Eichler EE, Sahinalp SC: **Combinatorial algorithms for structural variation detection in high-throughput sequenced genomes.** *Genome research* 2009, **19**:1270-1278.
12. Wang J, Mullighan C, Easton J, Roberts S, Heatley S, Ma J, Rusch M, Chen K, Harris C, Ding L, Holmfeldt L, Payne-Turner D, Fan X, Wei L, Zhao D, Obenaus J, Naeve C, Mardis E, Wilson R, Downing J, Zhang J: **CREST maps somatic structural variation in cancer genomes with base-pair resolution.** *Nature Methods* 2011, **8**:652-654.
13. Alkan C, Coe BP, Eichler EE: **Genome structural variation discovery and genotyping.** *Nature reviews Genetics* 2011, **12**:363-376.
14. Greenman CD, Pleasance ED, Newman S, Yang F, Fu B, Nik-Zainal S, Jones D, Lau KW, Carter N, Edwards PA, Futreal PA, Stratton MR, Campbell PJ: **Estimation of rearrangement phylogeny for cancer genomes.** *Genome research* 2011.
15. Raphael BJ, Volik S, Collins C, Pevzner PA: **Reconstructing tumor genome architectures.** *Bioinformatics* 2003, **19 Suppl 2**:ii162-171.
16. Kim YK, Bae GU, Kang JK, Park JW, Lee EK, Lee HY, Choi WS, Lee HW, Han JW: **Cooperation of H2O2-mediated ERK activation with Smad pathway in TGF-beta1 induction of p21WAF1/Cip1.** *Cellular signalling* 2006, **18**:236-243.
17. McPherson A, Hormozdiari F, Zayed A, Giuliany R, Ha G, Sun MG, Griffith M, Heravi Moussavi A, Senz J, Melnyk N, Pacheco M, Marra MA, Hirst M, Nielsen TO, Sahinalp SC, Huntsman D, Shah SP: **deFuse: an algorithm for gene fusion discovery in tumor RNA-Seq data.** *PLoS computational biology* 2011, **7**:e1001138.
18. Wang K, Singh D, Zeng Z, Coleman SJ, Huang Y, Savich GL, He X, Mieczkowski P, Grimm SA, Perou CM, MacLeod JN, Chiang DY, Prins JF, Liu J: **MapSplice: accurate mapping of RNA-seq reads for splice junction discovery.** *Nucleic acids research* 2010, **38**:e178.
19. Chen K, Wallis JW, Kandoth C, Kalicki-Veizer JM, Mungall KL, Mungall AJ, Jones SJ, Marra MA, Ley TJ, Mardis ER, Wilson RK, Weinstein JN, Ding L: **BreakFusion: targeted assembly-based identification of gene fusions in whole transcriptome paired-end sequencing data.** *Bioinformatics* 2012, **28**:1923-1924.
20. Sboner A, Karpikov A, Chen GX, Smith M, Mattoon D, Freeman-Cook L, Schweitzer B, Gerstein MB: **Robust-Linear-Model Normalization To Reduce Technical Variability in Functional Protein Microarrays (vol 8, pg 5451, 2009).** *Journal of Proteome Research* 2010, **9**:636-636.
21. Bignell GR, Santarius T, Pole JC, Butler AP, Perry J, Pleasance E, Greenman C, Menzies A, Taylor S, Edkins S, Campbell P, Quail M, Plumb B, Matthews L, McLay K, Edwards PA, Rogers J, Wooster R, Futreal PA, Stratton MR: **Architectures of somatic genomic rearrangement in human cancer**

- amplicons at sequence-level resolution.** *Genome research* 2007, **17**:1296-1303.
22. Inaki K, Hillmer AM, Ukil L, Yao F, Woo XY, Vardy LA, Zawack KF, Lee CW, Ariyaratne PN, Chan YS, Desai KV, Bergh J, Hall P, Putti TC, Ong WL, Shahab A, Cacheux-Rataboul V, Karuturi RK, Sung WK, Ruan X, Bourque G, Ruan Y, Liu ET: **Transcriptional consequences of genomic structural aberrations in breast cancer.** *Genome research* 2011, **21**:676-687.
 23. Alkan C, Sajjadian S, Eichler EE: **Limitations of next-generation genome sequence assembly.** *Nature Methods* 2011, **8**:61-65.
 24. McPherson A, Wu C, Hajirasouliha I, Hormozdiari F, Hach F, Lapuk A, Volik S, Shah S, Collins C, Sahinalp SC: **Comrad: detection of expressed rearrangements by integrated analysis of RNA-Seq and low coverage genome sequence data.** *Bioinformatics* 2011, **27**:1481-1488.
 25. McPherson A, Wu C, Wyatt AW, Shah S, Collins C, Sahinalp SC: **nFuse: discovery of complex genomic rearrangements in cancer using high-throughput sequencing.** *Genome Research* 2012, **22**:2250-2261.
 26. Li H, Durbin R: **Fast and accurate short read alignment with Burrows-Wheeler transform.** *Bioinformatics* 2009, **25**:1754-1760.
 27. Edgren H, Murumagi A, Kangaspeska S, Nicorici D, Hongisto V, Kleivi K, Rye IH, Nyberg S, Wolf M, Borresen-Dale AL, Kallioniemi O: **Identification of fusion genes in breast cancer by paired-end RNA-sequencing.** *Genome biology* 2011, **12**.
 28. Kim D, Salzberg SL: **TopHat-Fusion: an algorithm for discovery of novel fusion transcripts.** *Genome biology* 2011, **12**:R72.
 29. Wang J, Mullighan CG, Easton J, Roberts S, Heatley SL, Ma J, Rusch MC, Chen K, Harris CC, Ding L, Holmfeldt L, Payne-Turner D, Fan X, Wei L, Zhao D, Obenaus JC, Naeve C, Mardis ER, Wilson RK, Downing JR, Zhang J: **CREST maps somatic structural variation in cancer genomes with base-pair resolution.** *Nature Methods* 2011, **8**:652-654.
 30. Asmann YW, Hossain A, Necela BM, Middha S, Kalari KR, Sun Z, Chai HS, Williamson DW, Radisky D, Schroth GP, Kocher JP, Perez EA, Thompson EA: **A novel bioinformatics pipeline for identification and characterization of fusion transcripts in breast cancer and normal cell lines.** *Nucleic acids research* 2011, **39**:e100.
 31. Agarwal N, Adhikari AS, Iyer SV, Hekmatdoost K, Welch DR, Iwakuma T: **MTBP suppresses cell migration and filopodia formation by inhibiting ACTN4.** *Oncogene* 2012.
 32. Montero JC, Seoane S, Ocana A, Pandiella A: **P-Rex1 participates in Neuregulin-ErbB signal transduction and its expression correlates with patient outcome in breast cancer.** *Oncogene* 2011, **30**:1059-1071.
 33. Sosa MS, Lopez-Haber C, Yang C, Wang H, Lemmon MA, Busillo JM, Luo J, Benovic JL, Klein-Szanto A, Yagi H, Gutkind JS, Parsons RE, Kazanietz MG: **Identification of the Rac-GEF P-Rex1 as an essential mediator of ErbB signaling in breast cancer.** *Molecular cell* 2010, **40**:877-892.
 34. **Comprehensive molecular portraits of human breast tumours.** *Nature* 2012, **490**:61-70.

35. Robinson DR, Kalyana-Sundaram S, Wu YM, Shankar S, Cao X, Ateeq B, Asangani IA, Iyer M, Maher CA, Grasso CS, Lonigro RJ, Quist M, Siddiqui J, Mehra R, Jing X, Giordano TJ, Sabel MS, Kleer CG, Palanisamy N, Natrajan R, Lambros MB, Reis-Filho JS, Kumar-Sinha C, Chinnaiyan AM: **Functionally recurrent rearrangements of the MAST kinase and Notch gene families in breast cancer.** *Nature medicine* 2011, **17**:1646-1651.
36. **A map of human genome variation from population-scale sequencing.** *Nature* 2010, **467**:1061-1073.
37. Roychowdhury S, Iyer MK, Robinson DR, Lonigro RJ, Wu YM, Cao X, Kalyana-Sundaram S, Sam L, Balbin OA, Quist MJ, Barrette T, Everett J, Siddiqui J, Kunju LP, Navone N, Araujo JC, Troncoso P, Logothetis CJ, Innis JW, Smith DC, Lao CD, Kim SY, Roberts JS, Gruber SB, Pienta KJ, Talpaz M, Chinnaiyan AM: **Personalized oncology through integrative high-throughput sequencing: a pilot study.** *Science translational medicine* 2011, **3**:111ra121.
38. Ding L, Ley T, Larson DE, Miller CA, Koboldt DC, Welch JS, Ritchey JK, Young MA, Lamprecht T, McLellan MD, McMichael JF, Wallis J, Lu C, Shen D, Harris CC, Dooling DJ, Fulton RS, Fulton LL, Chen K, Schmidt H, Kalicki-Veizer J, Magrini V, Cook L, McGrath SD, Vickery TL, Wendl MC, Heath S, Watson MA, Link DC, Tomasson MH, et al: **Clonal evolution in relapsed acute myeloid leukaemia revealed by whole-genome sequencing.** *Nature* 2012.
39. Navin N, Kendall J, Troge J, Andrews P, Rodgers L, McIndoo J, Cook K, Stepansky A, Levy D, Esposito D, Muthuswamy L, Krasnitz A, McCombie WR, Hicks J, Wigler M: **Tumour evolution inferred by single-cell sequencing.** *Nature* 2011, **472**:90-94.
40. Pevzner P: *Computational molecular biology: An algorithmic approach.* Cambridge, MA: MIT Press; 2000.
41. Handsaker RE, Korn JM, Nemesh J, McCarroll SA: **Discovery and genotyping of genome structural polymorphism by sequencing on a population scale.** *Nature Genetics* 2011, **43**:269-276.

Figure legends

Figure 1 Schematic overview of BreakTrans. Plotted as an example are 3 genes *A*, *B* and *C* that range from genomic positions (black nodes) *a* to *c*, from *d* to *g*, and from *h* to *j*, respectively. Each gene contains two exons (arrow boxes) that can be transcribed from 5' to 3'. Gene *A* is on the positive (+) strand, while gene *B* and *C* are on the negative (-) strand. Two sets of putative novel genomic breakpoints are identified from alignments: $b+|e+$ between genomic positions *b* and *e* on the same strands by GSR predictor 1 (red), and $f+|i-$ between *f* and *i* on opposite strands by GSR predictor 2 (orange). Putative fusions are identified between exons *A1* and *C2* by fusion predictor 1, between exons *C1* and *A2* by fusion predictor 2, and between exons *B1* and *A1* by fusion predictor 3. Based on the plotted breakpoint graph and the locations and the orientations of exons, BreakTrans determines that the only genomically validated fusion is *A1*>*C2* (highly in blue), supported by a novel genomic allele $a+|b+|e+|f+|i-|h-$ that involves 2 novel genomic breakpoints and 3 genes.

Figure 2 Copy number profile in the SK-BR-3 genome. Plotted are three gene fusions predicted by BreakTrans (a) *PREX1*>*CPNE1*, (b) *MTBP*>*SAMD12*, (c) *WDR67*>*ZNF704*. The X axis represents genomic positions and Y axis represents absolute copy number in non-overlapping 10kb windows. The vertical red lines mark the locations of the GSR breakpoints that led to these fusions.

Figure 3 Breakpoints of novel fusions in SK-BR-3. (a) The novel tumor allele supporting *PREX1*>*CPNE1* consists of the first 3 exons of *PREX1* (green), an intronic segment of *PHF20* (orange) and the last 3 exons of *CPNE1* (blue). The RNA *PREX1*>*CPNE1* breakpoint between exons *A* and *B* was nominated by deFuse, while the genomic breakpoints SV1 and SV2 were detected by CREST. (b) Six genomic breakpoints from 3 gene fusions were selected for PCR validation (Additional File 8). SV1 and SV2 are from *PREX1*>*CPNE1*, SV3 and SV4 from *MTBP*-*SAMD12*, and SV5 and SV6 from *WDR67*-*ZNF704*. Clean PCR bands were observed at SV1, SV2, SV3 and SV6.

Figure 4 Definition of breakpoints and breakpoint strings. For intra-chromosome rearrangements, 4 types of breakpoints: (a) null, (b) jump, (c) inverse and (d) repeat between genomic positions x and y can be created that involves DNAs on either the positive (red arrow) or the negative (blue arrow) strands. A number (e.g., 3) is labeled on the edges to represent confidence scores (e.g., number of supporting reads) for the predicted adjacency. Edges without number or with the number “0” represent reference adjacency (null breakpoints). For inter-chromosomal rearrangements, 4 possible novel alleles (e) A-D, (f) B-C, (g) A-B and (h) C-D can be created by joining 4 breakends (A, B, C, D) from two wild-type alleles (A-C, B-D) through genomic breakpoints x and y . Each allele can be represented in 2 different orientations involving combinations of either the positive (red arrow) or the negative (blue arrow) strands. Breakpoint strings corresponding to above configurations are listed in the following table (i), in which + represents the positive strand and – the negative strand. Syntax of breakpoint strings is further explained in the **Methods**.

Table 1 Fusion genes and breakpoint paths predicted by BreakTrans-0.0.6

Eight gene fusions were predicted by BreakTrans-0.0.6, including 6 previously known fusions (#1-6) and 2 novel ones (#7-8). Four previously known fusions (#9-12) were not predicted due primarily to lack of coverage. For each fusion, at least one underlying genomic allele is found, represented as a breakpoint path that consists of a serial of breakpoint strings (**Methods**). '>' represents the predicted (5' to 3') order of a gene fusion.

#	Fusion Genes	Breakpoint Paths
1	<i>ANKHD1-EIF4EBP3>PCDH1</i>	• 5:139807117+65 5:141217466-
2	<i>CCDC85C>SETD3</i>	• 14:99059254-7 14:98966917-
3	<i>RARA>PKIA</i>	• 17:35727917+45 8:79637984+
4	<i>SUMF1>LRRFIP2</i>	• 3:4338455-34 3:37158400-
5	<i>TATDN1>GSDMB</i>	• 8:125618280-93 17:35321200-
6	<i>WDR67>ZNF704</i>	• 8:81882283-4 8:81882470+0 8:81916434+18 8:124171162-0 8:124158930-36 8:124161970+ • 8:124171162+18 8:81916434-
7	<i>MTBP>SAMD12</i>	• 8:121547851+33 8:119503797+0 8:119661057+2 8:119666167-0 8:119662603-33 8:118985543+0 8:118990300+28 8:118992237-0 8:118985543-33 8:119662603+0 8:119666167+2 8:119661057-
8	<i>PREX1>CPNE1</i>	• 20:46795673-17 20:33925625-0 20:33923847-18 20:33679982-
9	<i>DHX35-ITCH</i>	
10	<i>NFS1-PREX1</i>	
11	<i>CYTH1-EIF3H</i>	
12	<i>CSE1L-ENSG00000236127</i>	

Additional Material

Additional File 1: a list of 3,498 candidate gene fusion breakpoints in SK-BR-3, used as input to BreakTrans

Additional File 2: a list of 41,615 candidate genomic breakpoints in SK-BR-3, used as input to BreakTrans

Additional File 3: a list of 40 genomically validated fusion breakpoints output by BreakTrans-0.0.6

Additional File 4: a list of 1,994 candidate gene fusions predicted by nFuse-0.1.4

Additional File 5: Figures: S1, *PREX1-CPNE1* fusion detected from SK-BR-3 WTS data; S2-S5, integrative genomics views (IGV) of read alignments at the 2 GSR breakpoints (4 breakends) underlying *PREX1-CPNE1*; S6-S9, IGV of GSR breakpoints underlying *MTBP-SAMD12*; S10-S11, IGV of GSR breakpoints underlying *WDR67-ZNF704*; S12, whole genome somatic copy number alteration (log₂) of A09I; S13, the *NF1-NLE1* fusions detected in A09I; S14, somatic copy number alteration on Chr17 of A09I with red vertical lines marking the GSR breakpoints that support the *NF1-NLE1* fusion; S15-S18, IGV of the 2 GSR breakpoints (4 breakends) that underlie *NF1-NLE1*; S19, the *PPP1R1B-PIPOX* fusion detected in A0D1; S20, whole genome somatic copy number alteration (log₂) of A0D1; S21, somatic copy number alteration on Chr17 of A0D1 with red vertical lines marking the GSR breakpoints that support the *PPP1R1B-PIPOX* fusion; S22-27, IGV of the 3 GSR breakpoints (6 breakends) that underlie *PPP1R1B-PIPOX*; S28, the *PPP3R1-TTC27* fusion detected in A0YG; S29, whole genome somatic copy number alteration (log₂) of A0YG; S30, somatic copy number alteration on Chr2 of A0YG with red vertical lines marking the GSR breakpoints that support the *PPP3R1-TTC27* fusion; S31, zoomed-in view of S29 at the chr2 chromothripsis that harbors the fusion; S32-37, IGV of the 3 GSR breakpoints (6 breakends) that underlie *PPP3R1-TTC27*; S38-41, PCR validation of TCGA BRCA genomic breakpoints; S42, capillary sequencing trace of a PCR product that was not visible in the gel.

Additional File 6: a list of 124 fusion breakpoints (42 gene pairs) produced by Tophat-fusion from the validation RNA-seq data

Additional File 7: a list of 115 fusion breakpoints (62 gene pairs) produced by BreakFusion-1.0.1 from the validation RNA-seq data

Additional File 8: breakpoints and PCR primers for SK-BR-3 validation

Additional File 9: a list of 177 gene fusions and corresponding genomic breakpoints produced by BreakTrans from 43 TCGA breast cancer samples

Additional File 10: experimental design for validating 20 TCGA GSR breakpoints

Additional File 11: PCR validation of 20 TCGA GSR breakpoints in 9 TCGA samples

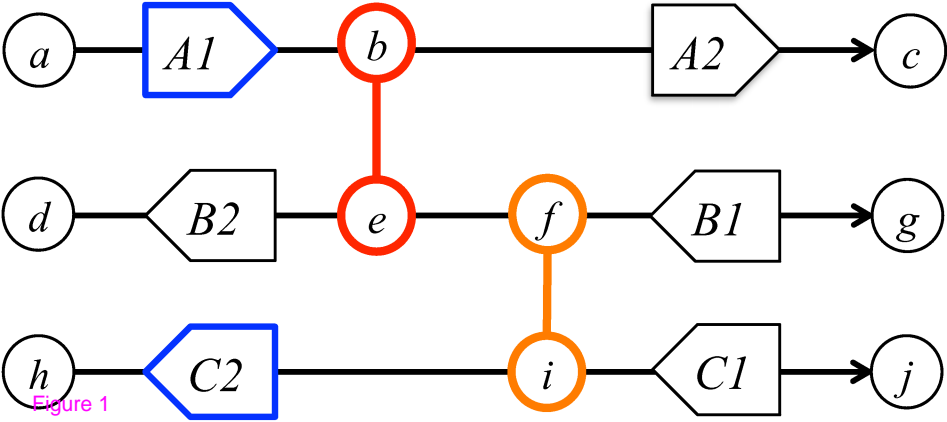
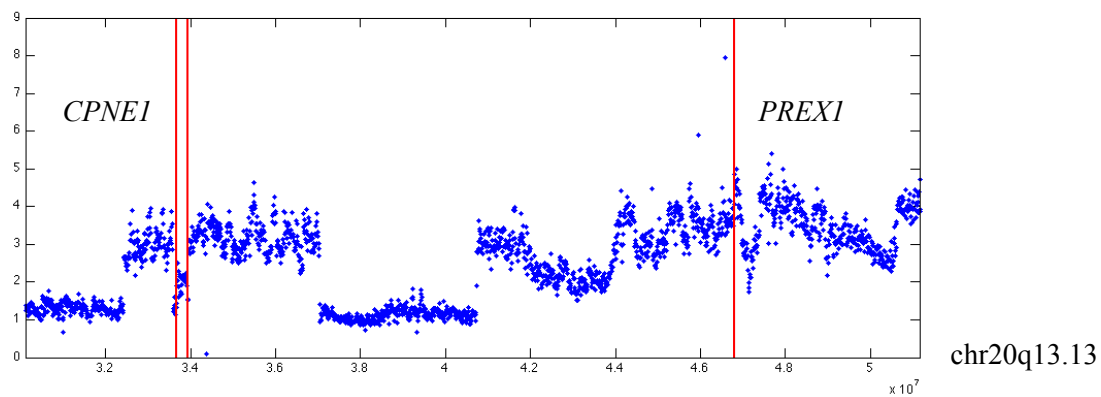


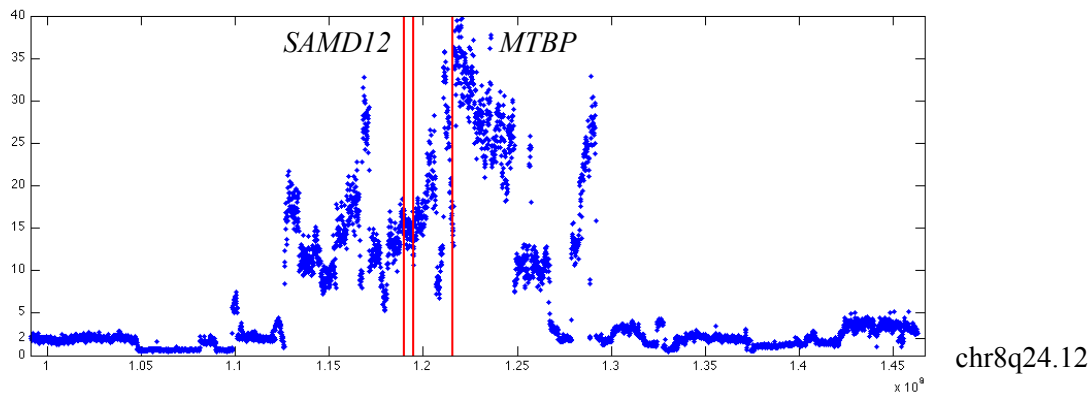
Figure 1

Fig. 2

a



b



c

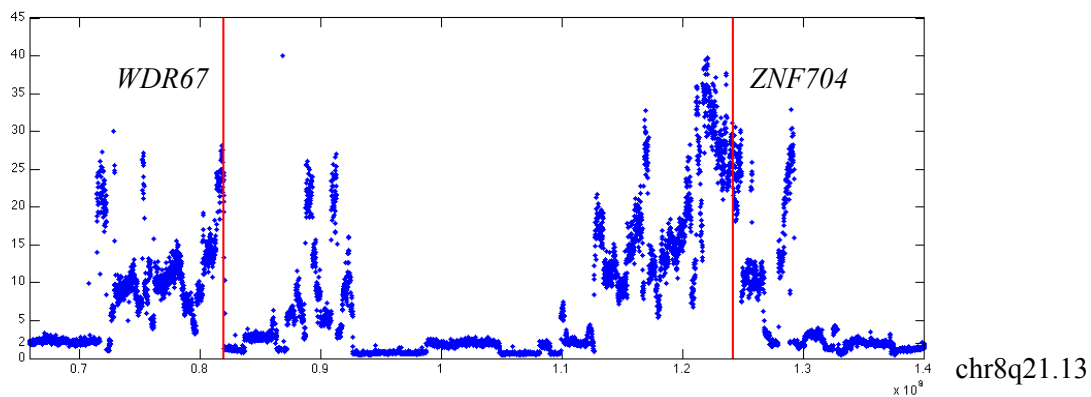


Figure 2

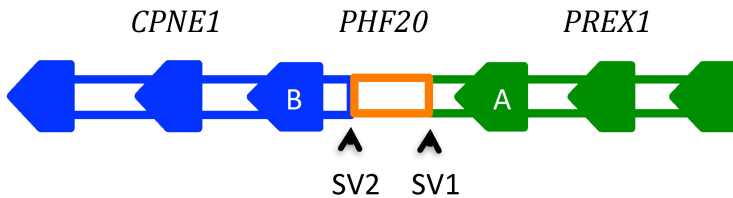
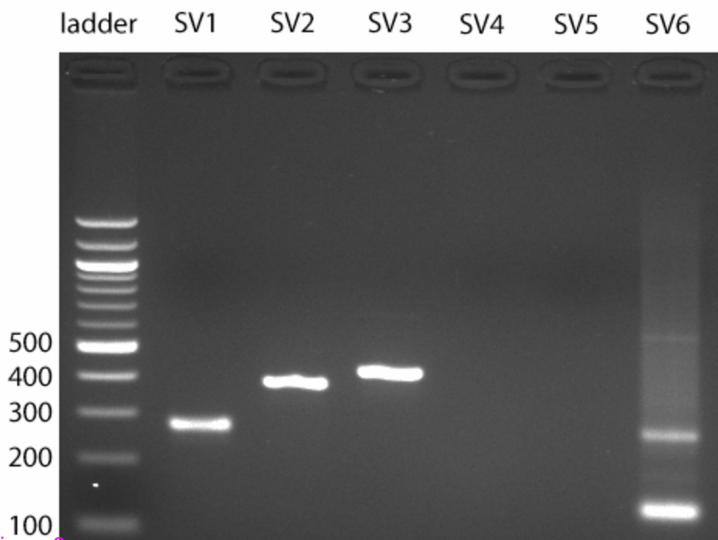
a**b**

Figure 3

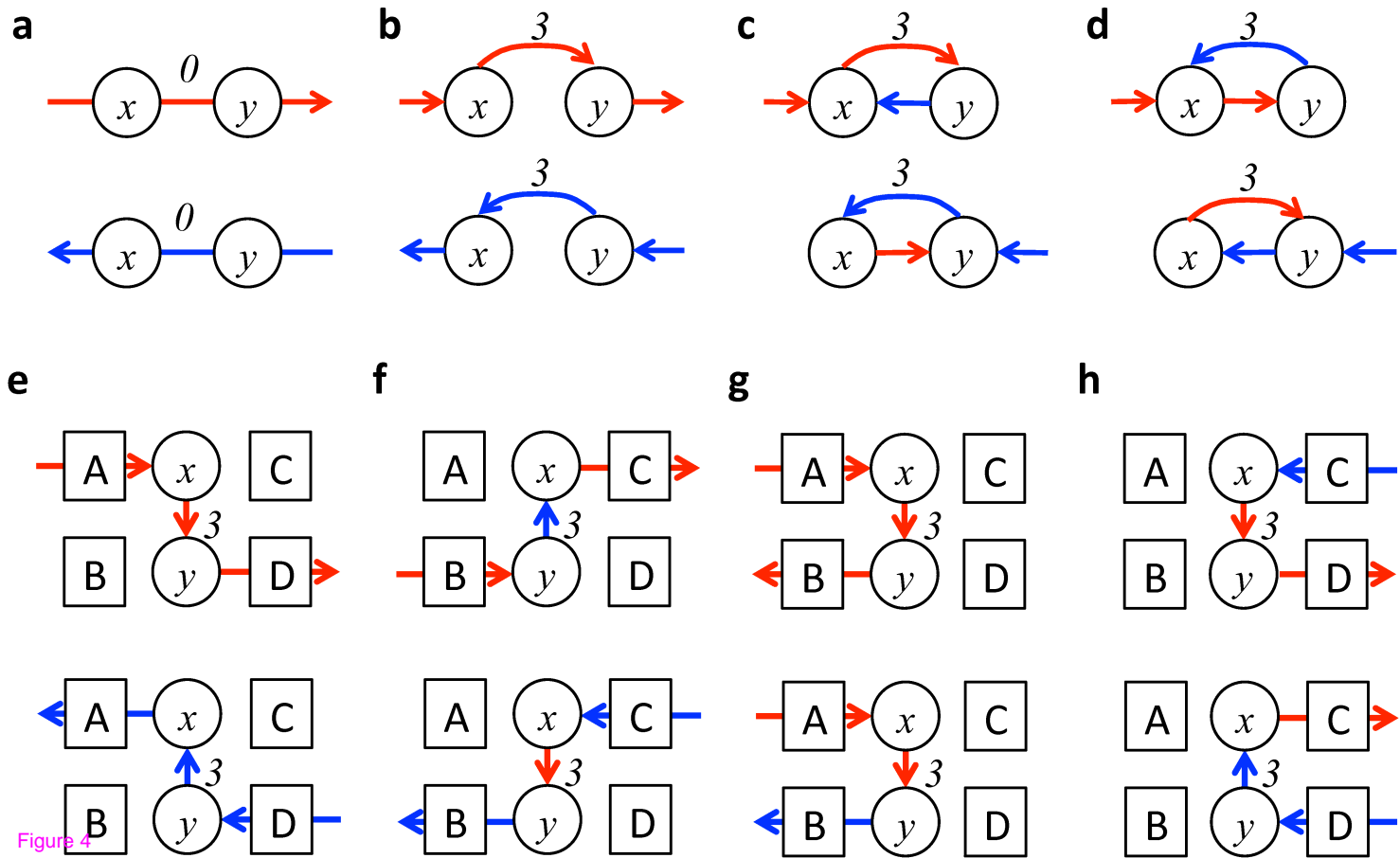


Figure 4

Rearrangement types	Breakpoint strings
a. null	$x+0 y+, y-0 x-$
b. jump	$x+3 y+, y-3 x-$
c. inverse	$x+3 y-, x-3 y+, y+3 x-, y-3 x+$
d. repeat	$y+3 x+, x-3 y-$
e. A-D	$x+3 y+, y-3 x-$
f. B-C	$y+3 x+, x-3 y-$
g. A-B	$x+3 y-, y+3 x-$
h. C-D	$x-3 y+, y-3 x+$

Additional files provided with this submission:

Additional file 1: Additional_File1.tsv, 153K

<http://genomebiology.com/imedia/1835681834106174/supp1.tsv>

Additional file 2: Additional_File2.tsv, 4027K

<http://genomebiology.com/imedia/1825232724106174/supp2.tsv>

Additional file 3: Additional_File3.tsv, 3K

<http://genomebiology.com/imedia/1498369623106174/supp3.tsv>

Additional file 4: Additional_File4.tsv, 1456K

<http://genomebiology.com/imedia/1056438377106174/supp4.tsv>

Additional file 5: Additional_File5.pptx, 4627K

<http://genomebiology.com/imedia/1819837128106174/supp5.pptx>

Additional file 6: Additional_File6.txt, 8K

<http://genomebiology.com/imedia/1725232574106174/supp6.txt>

Additional file 7: Additional_File7.tsv, 5K

<http://genomebiology.com/imedia/1410700468106174/supp7.tsv>

Additional file 8: Additional_File8.xlsx, 47K

<http://genomebiology.com/imedia/2307526141061749/supp8.xlsx>

Additional file 9: Additional_File9.xlsx, 63K

<http://genomebiology.com/imedia/9273150751061749/supp9.xlsx>

Additional file 10: Additional_File10.xlsx, 52K

<http://genomebiology.com/imedia/6047645721061749/supp10.xlsx>

Additional file 11: Additional_File11.xlsx, 10K

<http://genomebiology.com/imedia/1478244431061749/supp11.xlsx>